agriculture

MDPI

Article

Phenotypic Analysis and Gene Cloning of a New Allelic Mutant of *SPL5* in Rice

Ping Li [1,†], Nana Xu [1,†], Yang Shui [1,2], Jie Zhang [1,2], Wuzhong Yin [1,2], Min Tian [1], Faping Guo [3], Dasong Bai [1], Pan Qi [1], Qingxiong Huang [1], Biluo Li [1], Yuanyuan Li [1], Yungao Hu [1,2,*] and Youlin Peng [1,2,*]

[1] School of Life Science and Engineering, Southwest University of Science and Technology, Mianyang 621010, China; liping217@sohu.com (P.L.); xunana0502@163.com (N.X.); christinashui@163.com (Y.S.); zhangjie123@swust.edu.cn (J.Z.); ywz191665587@126.com (W.Y.); 18781629720@163.com (M.T.); bds1260377152@163.com (D.B.); qp13243@163.com (P.Q.); 18882340957@163.com (Q.H.); lb13198089330@163.com (B.L.); 15567535092@163.com (Y.L.)
[2] Rice Research Institute, Southwest University of Science and Technology, Mianyang 621010, China
[3] Rice Research Institute, Sichuan Agricultural University, Chengdu 611130, China; guo19970906@163.com
* Correspondence: huyungao@swust.edu.cn (Y.H.); ylpeng@swust.edu.cn (Y.P.)
† These authors contributed equally to this work.

Abstract: This study was conducted on the lesion-mimic mutant *lm5*, which was produced by mutagenesis of WYJ21 (WT) using ethyl methane sulfonate (EMS). The mutant *lm5* was short in the seedling stage and displayed yellowish-brown disease-like spots on leaves that were yellowish-brown when the plant was at the tillering stage. The disease-like spots gradually grew larger as the plant grew until it reached maturity. Compared to WT, *lm5* had considerably reduced the plant height, ear panicle length, tiller number, and 1000-grain weight. A single recessive gene was found to be in control of *lm5*, according to a genetic study. It was physically located 245 kb apart between the RM21160 and RM180 markers on chromosome 7. Using RiceData and other websites, analyze and sequence potential gene candidates. Exon 7 of *LOC_Os07g10390* (*OsLM5*) was identified to have a mutation that changed the 1560 base from G to A, changing the 788 amino acids from Arg to Lys. The *OsLM5* gene was found to be a new allele of the *SPL5* gene, encoding the protein shear factor SF3b3. Studies showed that OsLM5 was localized in the nucleus, and *OsLM5* was significantly expressed in leaves. Reactive oxygen species (ROS) accumulation occurred in the leaves and roots of mutant *lm5*, and qPCR results showed abnormal expression of genes related to chloroplast development as well as significantly increased expression of genes related to aging and disease course. The *OsLM5* gene may have a significant impact on the regulation of apoptosis in rice cells.

Keywords: rice; lesion-mimic mutant; root; ROS; splicing factor 3b subunit 3; RT-qPCR

Citation: Li, P.; Xu, N.; Shui, Y.; Zhang, J.; Yin, W.; Tian, M.; Guo, F.; Bai, D.; Qi, P.; Huang, Q.; et al. Phenotypic Analysis and Gene Cloning of a New Allelic Mutant of *SPL5* in Rice. *Agriculture* **2023**, *13*, 1875. https://doi.org/10.3390/agriculture13101875

Received: 9 August 2023
Revised: 11 September 2023
Accepted: 20 September 2023
Published: 25 September 2023

1. Introduction

Rice is one of the important food crops in China [1], and its planting area accounts for more than 30% of the national food crop area [2]. During the growing process of rice, it is easy to be affected by external stress factors, such as climate, pests, diseases, etc. These elements lead to the abnormal physiological activities of rice and ultimately affect the yield and quality of rice. Lesion Mimic Mutant (LMM) is a type of mutant that is characterized by the spontaneous formation of disease-like spots mediated by programmed cell death (PCD) in the absence of pathogen infection, environmental stress, or mechanical damage [3–5]. On the leaves, leaf sheaths, stalks, or seed shells of plants, disease-like spots frequently manifest [6,7]. Early lesion-mimic mutants have been extensively reported in Arabidopsis thaliana rice [8], maize [9], barley [10], wheat [11], tomato [12], and other crops, with ongoing research. Meanwhile, it was found that most of the lesion-mimic mutants were related to plant disease resistance, showing increased expression of defense-related genes and activation of defense-related pathways. It exhibits heightened resistance to

specific pathogens [13], and the lesion-mimic mutants are regarded as important materials for studying the molecular mechanism of plant resistance, which is of great significance for clarifying the molecular mechanism of plant resistance to external stresses such as diseases and pests and also providing support for the breeding of high-resistance improved varieties [14,15].

It was discovered that there were great differences in the shape and color of disease-like spots in different mutants. *Spl36* [16] and *spl*(Y181) [17] showed irregular shapes, while *spl24* [18,19] had regular shapes. The disease-like spots of *SPL3* [20] and *spl16* [21] were black, and those of *spl18* [22] and *lil1* [23] were reddish brown. In addition, the stage of appearance of disease-like spots is also different, as *spl2* [24], *spl3* [20], and other lesion-mimic mutants will show disease-like spots at the seedling stage. The *spl6* [25] mutant does not show the phenotype of disease-like spots until the tiller stage and the booting stage. With the growth and development of the plant, the phenotype of the lesion-mimic mutant will become more and more severe and even spread to the whole plant.

The occurrence of regulatory disease-like spots in rice is influenced by a variety of factors. With the mining, cloning, and functional research of more and more genes related to these phenotypes, the mechanism of their occurrence is gradually understood. Important signaling molecules called reactive oxygen species (ROS) are primarily formed in organelles, including plant mitochondria, plasma membranes, chloroplasts, peroxisomes, etc. Each plant cell has a redox pathway regulated by ROS, which regulates the physiological processes of cells, including gene expression, aging and death, and metabolism. The hydrogen peroxide (H_2O_2) produced by the respiratory chain and enzymatic reactions in mitochondria will be transferred to the peroxisome and finally transported to the nucleus and cytoplasm. The H_2O_2 formed in chloroplasts will eventually enter the nucleus and cytoplasm [26]. PCD, which is closely related to hypertensive response (HR) [27], can be caused by ROS. Studies have found that the Arabidopsis gene *Lsd1* is a member of the LSD1-like gene family, and its mutant *lsd1* shows disease-like spots. The mutation of this gene will cause the PCD and associated defense mechanisms to be activated [28]. Zeng et al. [29] studied that ubiquitin ligase E3, a protein encoded by rice Spl11, negatively regulates PCD and immune function in plants. Thus, it was found that the formation of disease-like spots in plants was accompanied by PCD [30]. Excessive ROS accumulation will cause damage to plant cells and eventually lead to cell death [31].

ROS can influence the development of disease-like spots in two separate ways. First, they can react with a large number of biomolecules, causing irreversible cell damage and ultimately cell death in plants [32,33]. In addition, ROS can also disrupt signal transduction pathways and alter gene expression. Studies have found that ROS plays a crucial role in pathogen defense, gene expression, and cell signal transduction in response to a variety of pathogens [34]. Excessive accumulation of superoxide free radicals (O_2) and H_2O_2 in plants can disrupt the redox balance in cells and lead to severe oxidative damage to nucleic acids, proteins, and lipid membranes [35,36]. In addition, the accumulation of ROS is closely related to the occurrence of PCD. For instance, the formation of Arabidopsis [37], wheat [38], rice [39,40], and other disease-like spots is accompanied by the accumulation of ROS and the occurrence of PCD. SPL33, encoding the eEF1A protein, contains one non-functional zinc finger domain and three functional EF-Tu domains. Wang et al. [41] found that the loss of SPL33 function leads to the accumulation of H_2O_2, accelerated leaf aging, and PCD, and finally produces reddish-brown lesions. ROS not only affects the formation of disease-like spots but also plays an important role in root growth and lateral root formation [42–44]. ROS production and related signaling pathways are involved in root formation [45,46]. Tsukagoshi [42] and Silva-Navas [43] found that primary root growth was strictly regulated by the differential accumulation of ROS at the apex. UPBEAT1 (UPB1) transcription factor is independent of the auxin pathway by inhibiting peroxidase gene expression in roots and regulating the distribution of H_2O_2 and O^{2-} in the root elongation region and meristem [42]. Therefore, the study of the characteristics and regulatory mechanisms of rice lesion-mimic mutants is helpful in revealing the molecular mechanism of PCD in plants.

In this study, *Wuyunjing21* was mutated by EMS to identify a mutant named *lm5*. The mutant was short in plant height and had brown disease-like spots on leaves at the tillering stage. This gene encodes the protein shear factor SF3b3. We identified the mutant gene and discovered that the lesion-mimic phenotype of the *lm5* mutant was caused by the single base mutation of the *OsLM5* gene, which is an allele of the *OsLM5* gene and the *SPL5* gene [47]. Mutations in the *OsLM5* gene disrupt the ROS balance in cells, disrupt the structure of chloroplasts, and lead to local cell death at the lesion mimic. The results suggest that *OsLM5* plays an important role in regulating PCD and ROS balance in rice.

2. Materials and Methods

2.1. Plant Materials and Growing Conditions

Lm5 mutants were obtained from the *Wuyunjing21* (WYJ21, WT) population by EMS mutagenesis. All the plants were grown in April 2022 in the paddy field at Southwest University of Science and Technology and in October 2022 in Lingshui, Hainan, under the natural conditions of 28~37 °C. Field management follows standard agricultural practices. Tests related to roots were completed in March 2023, measuring rice roots after 15 days of growth. The cultivation condition of rice was 14 h light/10 h dark, and the light intensity was 1200 μmol photons $m^{-2} \cdot s^{-1}$.

2.2. Investigation of Chlorophyll Content

The leaves of WTand mutant *lm5* at the tillering stage were collected, and chlorophyll (Chl) content was determined. The concentrations of carotenoids (Car), chlorophyll a (Chla), and chlorophyll b (Chlb) were determined by spectrophotometry using the method described by Wellburn [48]. Simply put, the leaf samples were cut into pieces of about 0.5 cm, soaked in 80% acetone, and treated in dark conditions for more than 24 h. The optical density (OD) of the extracts was measured by spectrophotometry at 663, 646, and 470 nm, with three biological replicates measured per sample.

2.3. Determination of Various Antioxidant Indexes

Superoxide dismutase (SOD), peroxidase (POD), malondialdehyde (MDA), and catalase (CAT) from a catalase assay kit (visible light) were purchased from the Nanjing Jianjiancheng Bioengineering Institute. Enzyme activity is measured according to the methods in the manufacturer's instructions. All tests were carried out on leaves at the tillering stage and roots at the seedling stage.

2.4. Real-Time PCR Analysis

Total RNA was extracted from rice leaves using the TIANGEN RNAprep Pure Plant Kit and reverse-transcribed into cDNA using the Ecorry EvoM-MLV reverse transcription kit. The ACTIN gene was used as the internal reference gene, and the gene expression was detected by the SYBR Green Pro Taq HS premixed qPCR kit. There were three replicates per sample. The housekeeping gene we use is *Actin*, and the primers used in qRT-PCR analysis are shown in Supplementary Table S2.

2.5. Histochemical Label Staining

Nitrotetrazolium blue chloride (NBT) staining for superoxide anion accumulation and DAB staining for H_2O_2 accumulation were tested [49]. In simple terms, the sample is placed in diaminobenzidine (DAB) or NBT stain solution at 28 °C for staining, then all materials are decolorized in 95% ethanol at 70 °C until there is no chlorophyll, and then transferred to 70% glycerin for photographing. Trypan blue staining was used to detect cell death [18]. The sample was soaked in a basin blue stain solution and kept in the dark for more than 48 h, then all materials were decolorized in 95% ethanol at 70 °C and then transferred to 70% glycerin for photography.

The DCFH-DA, 2′,7′-Dichlorodihydrofluorescein diacetate (H2DCFDA) experimental scheme was modified according to Leshem's method [50]. The leaves of WT and mutant

lm5 growing in the same growth period were selected, and the leaves were cut into 1 cm for incubation. Chlorophyll autofluorescence and oxidation of H2DCFDA were observed by Nikon AXR laser confocal microscopy.

The roots of WT and mutant *lm5* at the seedling stage were fixed with FAA. After dehydration, transparency, and penetration, the samples were cut into thin slices with a Lycra slicer. After paraffin eluting with xylene, the slices were stained with aniline blue and then observed with a Lycra optical microscope.

2.6. Gene Mapping

In the genetic analysis, we hybridized with R498 using *lm5* as the maternal parent to obtain F1 offspring to self-breed and produce an F2 population. The phenotype of the F2 generation population was identified, genetic analysis was conducted, and 40 mutant phenotypic single strains were selected for mixing to obtain a mixing pool. Gene mapping was performed by mapping cloning analysis. We used the software Primer5 for primer design and the software SnapGene for sequence alignment and peak mapping. The RiceData (https://www.ricedata.cn/gene/ accessed on 17 March 2023) was used to search the genetic information. The primers used for gene mapping are shown in Supplementary Table S3.

2.7. Subcellular Localization

The full-length *OsLM5* coding sequence 4068 bp was inserted into PAN580-GFP to construct the 35S::OsLM5::GFP vector, and the nuclear marker and the constructed vector were transformed into rice protoplasts for transient expression. Fluorescence signals were observed using a Zeiss LSM700 laser-scanning confocal microscope. Primers are shown in Supplementary Table S4.

3. Results

3.1. Phenotypic Characteristics of Mutant lm5

The rice variety *Wuyunjing 21* (wild-type, WT) was mutated by EMS (ethyl methylsulfonate), and a leaf lesion mutant named *lm5* was identified. The mutant was short in plant size (Figure 1A). During the tillering stage, mutant *lm5* showed yellowish-brown lesions from the middle of the leaf to the tip of the leaf (Figure 1B,C). With the progress of growth and development, the leaf lesions of the mutant became more and more obvious. In addition, compared with WT, mutant *lm5* had lower plant height at maturity and shorter internode and panicle length than WT (Figure S1A,C), and the number of tillers, number of branches, stems, seed setting rate, number of grains per panicle, and 1000-grain weight were all decreased (Figure S1D–K). The grain width and length of *lm5* mutants were significantly smaller than those of WT (Figure S1B), suggesting that *lm5* mutations may indirectly affect grain size. These results indicated that the formation of disease-like spots seriously affected the growth and development of *lm5* mutants.

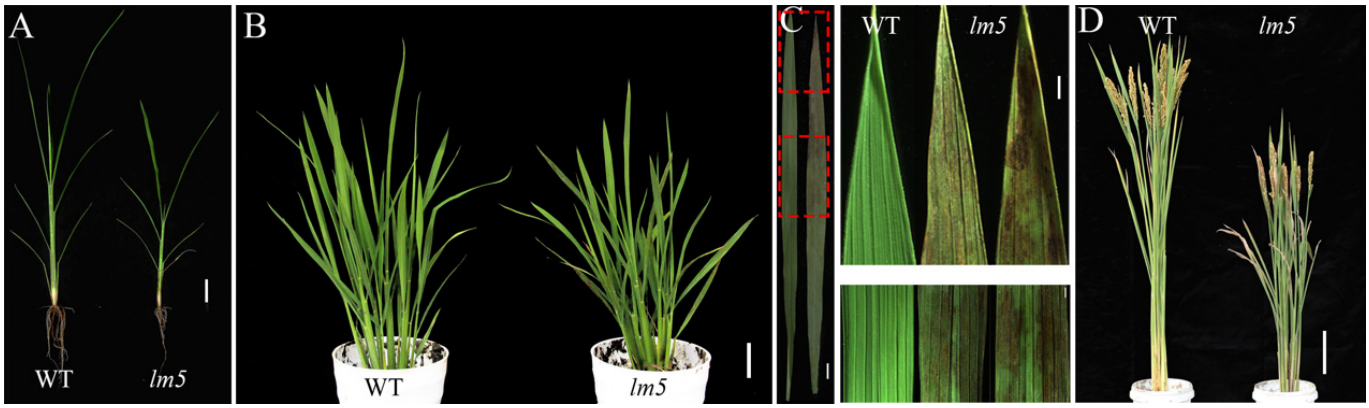

Figure 1. Phenotypic characteristics of lesion-mimic mutant *lm5*. (**A**,**B**) WT and *lm5* phenotypes at seedling and tillering stages, bar = 2 cm. (**C**) Phenotypes of WT and the disease-like spots of the *lm5* mutant in early tillering leaves, the red box is selected as the different phenotype at the tip and middle of the leaves of WT and the *lm5* mutant; on the right is an enlarged image, bar = 2 cm. (**D**) The whole phenotype of WT and mutant *lm5* at maturity, bar = 10 cm.

3.2. ROS Accumulation Occurred in lm5 Mutants

To further investigate the reason underlying the development of disease-like spots, we measured ROS levels in *lm5* mutants. Trypan blue (left in Figure 2A) and diaminobenzidine (right in Figure 2A) were used to stain the lesion sites of WT and *lm5* leaves. Leaves of mutant *lm5* were found to have an accumulation of dark blue and tan precipitates, which were not detected in WT leaves (Figure 2A). These results indicate that the occurrence of disease-like spots in *lm5* is accompanied by PCD and peroxide accumulation. To explore the accumulation of ROS in the leaves of mutant *lm5*, we measured the contents of H_2O_2 and MDA at the tillering stage (Figure 2B) and found that, compared with the WT, the concentrations of H_2O_2 and MDA in mutant *lm5* were significantly increased, and the accumulation of MDA would aggravate membrane damage [51]. Therefore, MDA content indirectly reflects the damage degree of mutant cells. We also measured the activities of CAT and POD (Figure 2B). The POD activity in the leaves of mutant *lm5* was lower than that of the WT, and the activity of ROS scavenging enzymes and CAT enzymes decreased. Abnormal ROS in the mutant and excessive accumulation of ROS and H_2O_2 may lead to the occurrence of disease-like spots in the leaves.

We incubated the leaves of WT and mutant *lm5* with an H2DCFDA fluorescent probe to detect ROS accumulation and distribution in tissues (Figure 2C). Observations under laser confocal microscopy showed that the probe's green oxidation state fluorescence signal was observed in *lm5* mutants but not in the WT.

Since ROS levels are strictly regulated by the antioxidant system, we detected the expression of genes related to ROS clearance and found that the expression levels of *AOX1a, AOX1b, APX2, SODA1,* and *CATB* genes were increased (Figure 2D). The high expression of ROS detoxification genes in mutant *lm5* may be caused by the elevated level of ROS in cells. Compared with WT, the expression levels of aging genes such as *OsWRKY2*, *OsWRKY7*, *OsNAC2,* and *SGR* in *lm5* mutants increased (Figure S2A), and the expression of disease-like spots course-related genes *PR10* and *JIOsPR10* increased significantly (Figure S2B). The above results indicate that the activity of ROS scavenging enzymes in *lm5* is reduced, the balance of the scavenging system is destroyed, resulting in a large accumulation of ROS, lipid peroxidation, increased MDA content, and finally cell damage resulting in the occurrence of disease-like spots.

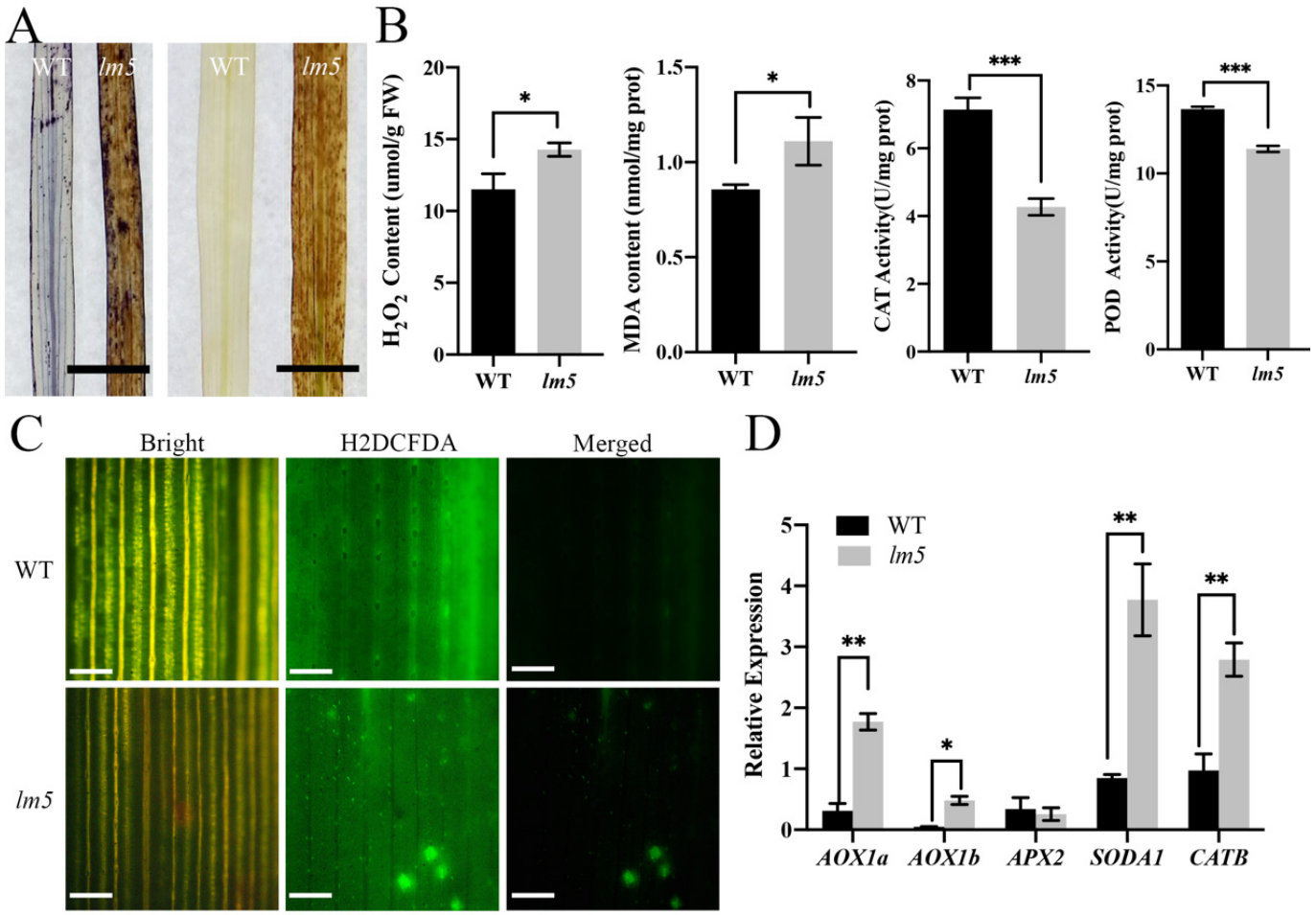

Figure 2. ROS accumulation in WT and *lm5* mutants. (**A**) Trypan blue and DAB staining of leaves of WT and mutant *lm5*, bar = 2 cm. (**B**) Determination of H_2O_2, MDA, CAT, and POD contents in WT and mutant *lm5*. (**C**) Microscopic observation of H2DCF-DA in WT and mutant *lm5*, with green representing oxidized H2DCFDA and red representing chlorophyll, bar = 20 μm. (**D**) Differences in ROS-related gene expression levels between WT and *lm5* at the tillering stage. *, $p < 0.05$; **, $p < 0.01$; ***, $p < 0.001$.

3.3. The Chlorophyll Content of the lm5 Mutant Decreased

The formation of disease-like spots caused the difference in leaf color, so the chlorophyll content of leaves was detected to determine whether it would affect the change in pigment. It was found that the contents of chlorophyll a, chlorophyll b, carotenoid, and total chlorophyll in the leaves of *lm5* at the tillering stage were significantly lower than those of WT. Among them, the chlorophyll content of mutant *lm5* was 39.2% lower than that of WT, the chlorophyll b content was 25.5% lower than that of WT, the total chlorophyll content was 39.7% lower than that of WT, and the carotenoid content of mutant *lm5* was 33% lower than that of WT. The results showed that the formation of disease-like spots in mutant *lm5* affected chlorophyll synthesis.

The leaf of mutant *lm5* has disease-like spots, and the chlorophyll content in the leaves is significantly reduced. The formation of disease-like spots in mutant *lm5* may lead to the destruction of chloroplast structure. We further quantitatively analyzed chloroplast-related genes and chlorophyll-related genes in the leaves. The expression of chloroplast genes depends on the activity of two RNA polymerases, plastid-encoded RNA polymerase (PEP) and nucleus-encoded RNA polymerase (NEP) [52,53]. *HSA1*, *OsFLN1*, *OsFLN2*, *OsTrxZ*, *POLP1*, *RpoA*, and *RpoB* belong to plastid-dependent RNA polymerase genes [54,55]. Through the analysis of chlorophyll gene expression, it was found that, compared with WT,

the expression of *NYC4* and *DVR* genes in the leaves of mutant *lm5* decreased while the expression of *NYC3* increased (Figure 3B), indicating that the change in chlorophyll content of the mutant may be caused by the destruction of the chloroplast structure of the mutant. Quantitative analysis showed that the expression levels of chloroplast development genes *HSA1*, *OsFLN2*, *OsTrxZ*, *POLP1*, and *FtsZ* increased (Figure 3C), indicating that the disturbance of chloroplast development gene expression interfered with PEP activity, thus affecting chloroplast development.

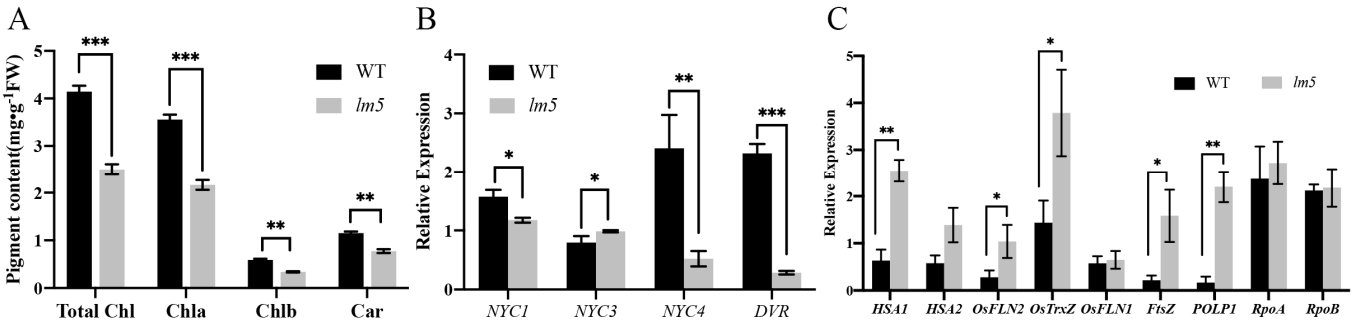

Figure 3. Analysis of the chlorophyll content difference between WT and *lm5* at the tillering stage. (**A**) Determination of chlorophyll content of WT, *lm5*, at the tillering stage. (**B**) Expression of WT and *lm5* and chlorophyll-related genes. (**C**) Expression of genes related to chloroplast development in WT and *lm5*. *, $p < 0.05$; **, $p < 0.01$; ***, $p < 0.001$.

3.4. Genetic Analysis and Candidate Gene Mapping of Macular Mutant lm5

To reveal the molecular mechanism behind the disease-like spots phenotype of the mutant *lm5*, we hybridized with R498 using *lm5* as the maternal parent to obtain F1 progeny for the self-breed F2 population. The phenotype of the F2 progeny population was identified, and genetic analysis was conducted. It was found that there were 978 normal strains and 342 mutant strains of *lm5*. The Chi-square test results show that the separation ratio is 3:1 ($\chi^2 = 0.58 < \chi^2_{0.05} = 3.84$), indicating that the phenotype of mutant *lm5* was controlled by a pair of recessive nuclear genes.

Linkage analysis of two parents of R498 and *lm5* was performed by designing polymorphic markers, and *lm5* was initially located between XT-1 and RM21309. A total of 320 recessive plaque single strains from the F2 population were used in this interval for fine localization by screening new polymorphism primers. It was found that there were three exchange single strains at RM21160 and two exchange strains at RM180. Finally, *lm5* was located between the markers RM21160 and RM180, with a physical distance of 245 kb (Figure 4A). By gramene, RiceData, and other websites analyzed the prediction analysis of genes in the 245 kb location interval and found that there were 33 annotated genes in the interval (Table S1). Of these, 16 encode expression proteins, and 14 genes have been annotated for possible functions; By analyzing the phenotypes of the genes encoding predicted splicing factor 3b subunit 3, encoding zeta-carotene dehydrogenase, and encoding cysteine-rich alcohol-soluble gluten of the reported genes, it was found that the phenotypes of the genes encoding predicted splicing factor 3b subunit 3 were similar to this gene. Therefore, WT and the mutant lm5 were sequenced (Figure 4B). A difference was found between WT and the mutant *lm5*, in which the 1560 base of exon 7 was mutated from G to A, resulting in a change in the 788 amino acids (Arg to Lys). At the same time, the F2 mutant material was also sequenced, which further confirmed that the gene had a single base mutation (Figure S3). Therefore, *LOC_Os07g10390* was taken as a candidate gene and named *OsLM5* (Lesion Mimic 5). The *OsLM5* gene was found to be an allele of the *SPL5* gene through analysis [47].

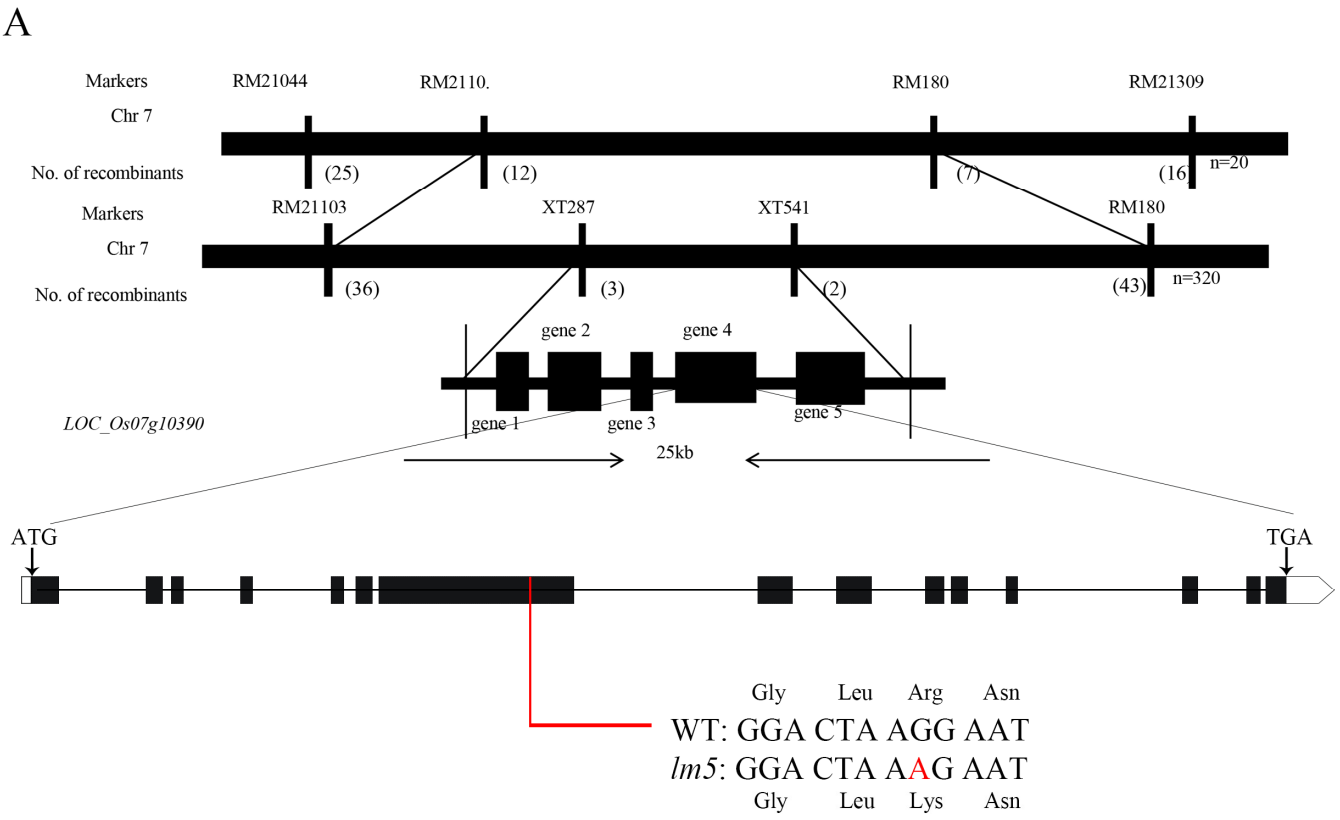

Figure 4. Candidate gene localization. (**A**) In mapping cloning and gene mapping of candidate genes, n = 20 was the initial population number; n = 320 is the number of fine localization populations. (**B**) Sequencing and identification of WT and *lm5* candidate genes. SnapGene for sequence alignment.

3.5. OsLM5 Expression Pattern Analysis

To understand the expression of the *OsLM5* gene in different tissues, we collected WYJ21 tissue materials and detected the expression level of the *OsLM5* gene by qRT-PCR. The *OsLM5* gene was found to have the highest expression level in leaf tissues (Figure 5A), followed by a higher expression level in roots, indicating that the *OsLM5* gene plays a major role in leaves. To determine the subcellular localization of the OsLM5 protein, we constructed a 35S::LM5::GFP vector and performed a transient transformation assay with nuclear marker-transformed rice protoplasts for co-expression. Confocal laser scanning microscopy showed that the GFP signal of the 35S::LM5::GFP fusion protein was co-located with the red fluorescence of nuclear markers in protoplasts (Figure 5B), and the OsLM5 protein may also play a role in the cytoplasm.

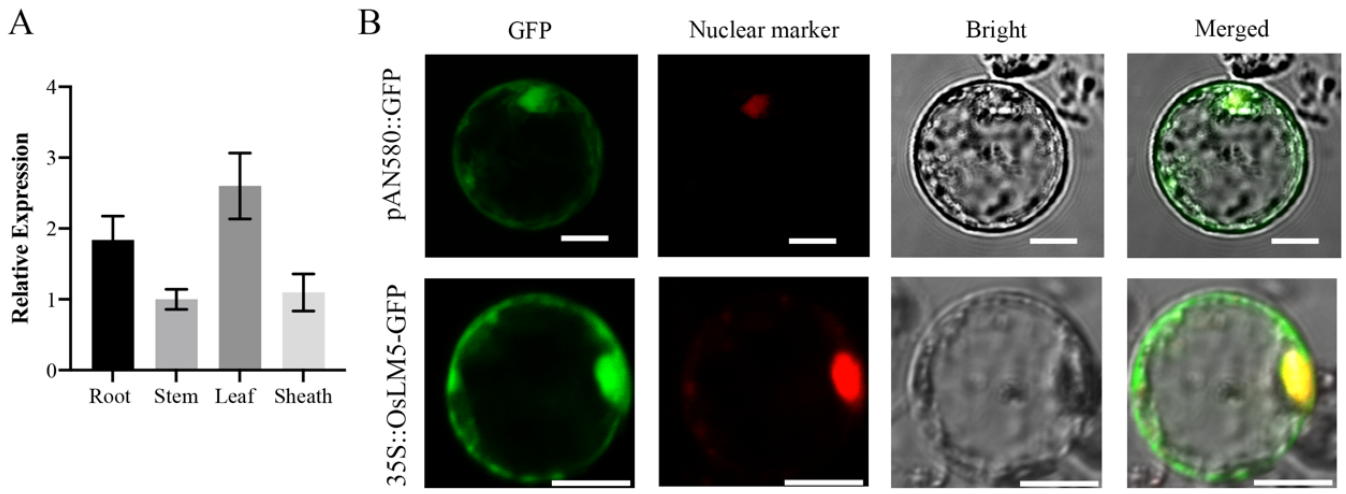

Figure 5. OsLM5 expression pattern analysis. (**A**) *OsLM5* expression profile analysis. (**B**) Subcellular localization of OsLM5 protein, bar = 10 μm.

3.6. OsLM5 Mutations Affect Root Development

Compared with WT, mutant *lm5* had short growth and short root length (Figures 6A and S4A,B). Expression profile analysis found that the *OsLM5* gene was active in roots (Figure 5A). Paraffin sections were performed on the roots of WT and mutant *lm5*, and obvious changes were found in root cell morphology. Compared with WT, the root cells of mutant *lm5* became smaller, the number of cells increased, and the size of single cells in the root crown, meristem zone, elongation zone, and mature zone decreased significantly (Figure S4D). Previous studies have found that ROS accumulation in roots can affect root growth. DAB and NBT staining were performed on taproots of WT and mutant *lm5*, and grayscale analysis of NBT staining was performed, and it was found that mutant *lm5* roots were dyed brown more deeply by DAB (Figure 6D). NBT staining and grayscale analysis showed that O^{2-} in mutant *lm5* roots was higher than WT (Figures 6E and S4E), indicating ROS accumulation in mutant *lm5*. The H_2O_2-related indexes of roots of WT and *lm5* were determined, and it was found that the H_2O_2 content and MDA content of mutant *lm5* were significantly higher than those of WT, the H_2O_2 scavenging ability of CAT and POD was significantly reduced (Figure 6F), and the catalytic capacity of SOD to generate H_2O_2 was significantly increased. *OsLM5* mutations lead to H_2O_2 accumulation in roots, which affects root development.

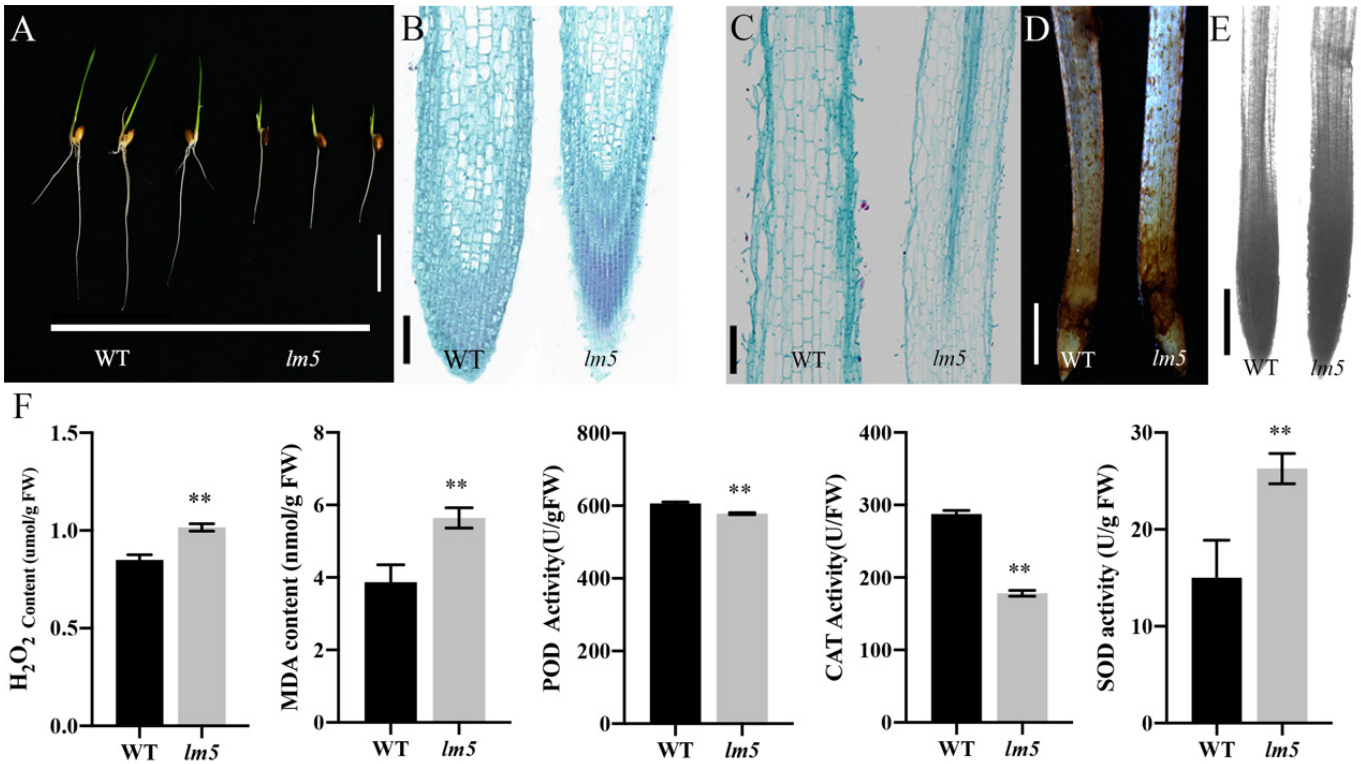

Figure 6. Root growth difference between WT and mutant *lm5* at the seedling stage. (**A**) Root phenotype of WT and mutant *lm5*, bar = 2 cm. (**B**,**C**) The root of WT and mutant *lm5* was observed in paraffin sections, bar = 100 μm. (**D**,**E**) The roots of WT and mutant *lm5* were stained with DAB and NBT, bar = 100 μm. (**F**) Determination of H_2O_2, MDA, POD, CAT, and SOD contents in the roots of WT and mutant *lm5* at the seedling stage. **, $p < 0.01$.

4. Discussion

4.1. The Formation of Leaf Lesions Affected the Agronomic Traits of Mutant lm5

The appearance of disease-like spots on rice leaves will reduce the chlorophyll content and photosynthetic rate of rice leaves, affect the photosynthesis and dry matter accumulation of rice leaves, and then affect the agronomic traits of rice mutants. Qiao et al. [56] reported that the chlorophyll content and photosynthetic system II efficiency of the spot-like mutant *spl28* decreased, and the yield decreased. Studies on the lesion-mimic mutant *lmm8* found that its chlorophyll content and PSII efficiency decreased, and the final thousand-grain weight and seed-setting rate were significantly reduced [57]. The main agronomic characters of *spl36*, such as plant height, effective panicle number, panicle length, kernel number per panicle, seed setting rate, and 1000-grain weight, were significantly decreased [6]. Ma et al. [58] studied the mottle leaf mutant *spl35* and found that due to the emergence of reddish-brown lesions, chloroplast development was abnormal, resulting in a decrease in the seed setting rate and 1000-grain weight of the mutant *spl35*. Consistent with the above studies, the mutant *lm5* appeared with yellow-brown lesions from the early tillering stage and lasted until maturity (Figure 1). Some agronomic traits of mutant *lm5*, such as plant height, effective panicle number, 1000-grain weight, and seed setting rate, were significantly lower than those of WT due to the appearance of disease-like spots, which ultimately led to a decrease in its yield (Figure S1).

4.2. ROS Accumulation Led to the Formation of Disease-like Spots in Mutant lm5

The accumulation of PCD and ROS around leaf lesions can lead to oxidative damage to plants, which is a way for plants to resist external infection [20,59]. Many studies have shown that plants have their own ROS clearance mechanism, and the production of ROS in plant cells is clearly in dynamic equilibrium to balance their own ROS [3,34,40]. ROS

accumulation has been detected in more than 40 kinds of rice lesion-mimic mutants that have been cloned [60]. A large amount of ROS accumulates around the leaf lesion of mutant *spl28* [56]. ROS within the normal range are important signals in response to stress, regulation of plant growth and development, and PCD [61]. Mutant *ell1* accumulated a large amount of ROS and a large amount of H_2O_2 accumulation, and the presence of dead cells was found in *ell1*. Gene expression related to oxygen binding and ROS clearance was upregulated. Abnormal PCD occurred in the ell1 mutant, and excessive ROS accumulation can mediate cell death [3]. Our study had similar results. Through the determination of Trypan blue and DAB staining on the leaves of mutant *lm5* and related physiological indexes (Figure 2A), it was found that a large number of ROS accumulated and cell death existed in the leaves of the lesion-mimic mutant, and the activities of CAT- and POD-related H_2O_2 protective enzymes were significantly reduced, while the activity of SOD, which catalyzed H_2O_2 generation, was significantly increased, possibly due to the increase in H_2O_2 content (Figure 2B). The clear mechanism of ROS is disturbed, and the cell structure is destroyed. The increase in MDA content aggravated the damage to the membrane of mutant leaves. At the same time, it was also found that there was cell death around the leaf lesions of mutant *lm5*, indicating that excessive accumulation of ROS caused the death of leaf cells.

ROS is a key signal in the process of plant root elongation and differentiation. Studies in Arabidopsis have shown that a decrease in O^{2-} concentration reduces root elongation, but the removal of H_2O_2 can promote root elongation [62]. *RITF1* overexpression can induce the ROS signal downstream of *RGF1* (enhanced O^{2-} signal in the meristem region) and promote root meristem development [60]. Interestingly, we also found an accumulation of ROS and O^{2-} in mutant *lm5* roots, which inhibited the root elongation of mutant *lm5*. The electron transport chain of plant mitochondria has multiple pathways, mainly the cytochrome pathway (CP) and alternative respiratory pathway (AP). The alternate respiratory pathway is a branch of the main respiratory chain that contains an alternative oxidase (AOX), the terminal oxidase in the respiratory chain [63], which is consumed in the form of heat energy to reduce oxidative damage, maintain oxidative balance in mitochondria, and limit the production of ROS [64]. AOX has an important relationship with stress resistance [65], resistance to high temperature stress [66], and maintenance of metabolic balance [67]. Related studies have reported that *AOX1a* and *AOX1b* [68] participate in alternate oxidase through respiration, and *APX2* [69] is related to the gene of ascorbate peroxidase, which mainly acts to clear ROS. *OsCATA* and *OsCATB* [70] are genes involved in the H_2O_2 metabolic pathway. In this study, aging, disease course, and ROS-related quantification were performed on the macular mutant *lm5*, and it was found that the expression of ROS genes *AOX1a*, *AOX1b*, *SODA1*, and *CATB* of the mutant were significantly up-regulated (Figure 2D), indicating that the accumulation of ROS in the mutant *lm5* induced the expression of *AOX1* and other genes to affect the occurrence of cyanogen-resistant respiration. At the same time, the expression levels of aging genes *OsWRKY2*, *OsWRKY7*, *OsNAC2*, and *SGR* were up-regulated, indicating that the accumulation of ROS could stimulate senescence-related mechanisms and accelerate the aging and death of plants. Due to the formation of disease-like spots, the plant's defense mechanism is activated, and the expression of *PR10*, *JIOsPR10*, and other resistance genes in mutant *lm5* is increased (Figure S2A,B). The mutation of *OsLM5* affects a series of resistance gene expressions in rice. Therefore, *OsLM5* is of great significance in theoretical research and disease-resistance breeding. The above studies indicated that the lesion-mimic mutant would be accompanied by ROS accumulation and cell death during the disease-like spot formation process, resulting in the phenotype of mutant *lm5*. *OsLM5* can regulate ROS metabolism in leaves and roots, thereby affecting the formation of leaf lesions and root elongation.

4.3. Effects of Mutant lm5 on Photosynthetic Function in Leaves

It was found that the chlorophyll content of rice spot-like mutant *spl41* gradually decreased with the increase of the spot-like phenotype, indicating that the formation of

disease-like spots would affect chlorophyll synthesis and lead to premature plant aging [71]. Ma et al. [57] found that the leaf mutant *spl35* with spotted leaves showed decreased pigment content and increased ROS accumulation. It was found that the phenotype of mutant *llm1* was induced by light, the content of photosynthetic pigment was significantly decreased, the number of chloroplasts in the mutant mesophyll cells was reduced, and the chloroplast structure was destroyed [13]. In this study, the chlorophyll content of the leaf after the formation of the morphed mutant *lm5* was detected, and it was found that the chlorophyll content of the mutant *lm5* was significantly lower than that of WT. In mutant *lm5*, chloroplast development genes *HSA1*, *OsFLN2*, *OsTrxZ*, *FtsZ*, *POLP1*, and other genes were up-regulated, and the expression of chlorophyll-related genes *NYC4* and *DVR* decreased while *NYC3* expression increased (Figure 3), indicating that the formation of disease-like spots in mutant *lm5* affected chloroplast development and chlorophyll synthesis. Chloroplast damage was caused by the leaf lesion of the mutant, which affected the normal photosynthesis of the plant.

4.4. OsLM5 Is a New Allele of SPL5

OsLM5 is a new allele of the *SPL5* gene encoding SF3b3, belonging to the SF3b3 splicing family. SF3b3, a 130-kDa protein, is a component of a multi-subunit complex identified as a splicing factor that required the addition of U2 snRNP during pre-spliceosome formation [72]. As an important component of the U2 snRNP, SF3b3 is involved in the recognition of pre-messenger RNA branch sites in the splice, which is crucial for the accurate excision of pre-messenger RNA introns in yeast [73]. Menon et al. [74] found that SF3b3 is related to the cullin-RING E3 ubiquitin ligase, which plays a role in stabilizing the genome during the cell cycle. Yamasaki et al. [75] found that SF3b3 can bind to C-type lectin in macrophages to form receptors, induce the production of some inflammatory cells, such as neutrophils, and enter damaged tissues to induce cell death. In mice, the SF3b3 gene can induce significant downregulation of the early sac apoptosis gene of the embryonic stem cell sac [76]. Chen et al. [47] discovered that the Spotted mutant Spotted leaf 5 (*spl5*), which appeared for the first time in rice, was missing a G-base in exon 7, leading to a frameshift mutation and an advanced stop codon. Ge et al. [77] discovered a new *spl5* allele, *OsSL5*, which has a single base mutation at site 3647, resulting in amino acid changes. The plant height, ear length, and stem number of the *sl5* mutant were significantly lower than those of the WT. *Sl5* mutants begin to develop disease-like spots at the tip of the leaf at the seedling stage, and these spots spread throughout the leaf as they grow [77]. In the later stages of growth, the size and number of spots increased further, and *SPL5* may be involved in the apoptosis of rice cells. The *lm5* mutant obtained in this study is a mottle leaf spot mutant, whose phenotype first appeared at the tillering stage and gradually expanded with the growth process until maturity. Our study found that the *OsLM5* gene may be involved in apoptosis regulation by encoding the SF3b3 protein. It is a new allelic mutant of *SPL5*, which has a single base mutation on the 1560th base of the gene, resulting in an amino acid change (Figure 4). The mutation site is located in an important conserved domain of the gene, so the single base mutation causes the mutant *lm5* to produce very severe disease-like spots. By studying roots, we found that this gene mutation can regulate the size of root cells through ROS (Figure 5 and Figure S4), indicating that OsLM5 not only affects the leaves' development but also affects the elongation of roots through ROS.

There have been no reports on the involvement of SF3b3 in rice defense response, and the specific regulatory mechanism of splicing involved in this gene in rice remains unclear and needs to be further explored. Therefore, *lm5* mutants can be used as an effective tool to study the regulatory mechanism of SF3b3 defense in plants and molecular breeding for crop disease resistance.

5. Conclusions

In this study, we discovered that mutations in the *OsLM5* gene disrupt the ROS balance in cells, disrupt the structure of chloroplasts, and lead to local cell death at disease-like

spots on leaves. *OsLM5* plays an important role in regulating cell death and ROS balance in rice. The *OsLM5* gene encodes the protein splicing factor SF3b3. Currently, there are no reports on the involvement of SF3b3 in defense responses in rice. The specific regulatory mechanism of splicing involved in this gene in rice remains unclear, and further exploration is needed. Therefore, *lm5* mutants can be used as an effective tool to study the regulatory mechanism of SF3b3 defense in plants and molecular breeding for crop disease resistance.

Supplementary Materials: The following supporting information can be downloaded at: https://www.mdpi.com/article/10.3390/agriculture13101875/s1. Figure S1: Agronomic traits of WT and mutant *lm5* at maturity; Figure S2: Expression of genes related to aging and disease progression; Figure S3: F2 generation sequencing analysis; Figure S4: Root differences between WT and mutant *lm5*; Table S1. Candidate genes of mutant *lm5*; Table S2. Primers used for qRT–PCR analysis in this study; Table S3. Primers for polymorphism screening; Table S4. Primers used for PCR amplification and plasmid constructions.

Author Contributions: Conceptualization, P.L. and N.X.; methodology, P.L. and M.T.; software, P.L., W.Y., J.Z. and Y.L.; validation, P.L., F.G., M.T., N.X., B.L. and Y.S.; formal analysis, P.L., M.T., P.Q., Q.H. and D.B.; investigation, P.L., N.X., M.T. and F.G.; resources, Y.P.; data curation, P.L. and N.X.; writing—review and editing, P.L.; visualization, P.L.; supervision, Y.P. and Y.H.; project administration, Y.P. and Y.H.; funding acquisition, Y.P. and Y.H. All authors have read and agreed to the published version of the manuscript.

Funding: This research was supported by the National Natural Science Foundation of China, Grant Number: 32001491; the Natural Science Foundation of Sichuan Province, Grant Number: 2022NSFSC0153; and the Key Research and Development Program of Sichuan, Grant Number: 2021YFYZ0016.

Institutional Review Board Statement: Not applicable.

Data Availability Statement: The data reported in this study are contained within the article.

Conflicts of Interest: The authors declare no conflict of interest.

References

1. Gross, B.L.; Zhao, Z. Archaeological and genetic insights into the origins of domesticated rice. *Proc. Natl. Acad. Sci. USA* **2014**, *111*, 6190–6197. [CrossRef] [PubMed]
2. Muthayya, S.; Sugimoto, J.D.; Montgomery, S.; Maberly, G.F. An overview of global rice production, supply, trade, and consumption. *Ann. N. Y. Acad. Sci.* **2014**, *1324*, 7–14. [CrossRef] [PubMed]
3. Cui, Y.; Peng, Y.; Zhang, Q.; Xia, S.; Ruan, B.; Xu, Q.; Yu, X.; Zhou, T.; Liu, H.; Zeng, D.; et al. Disruption of *EARLY LESION LEAF 1*, encoding a cytochrome P450 monooxygenase, induces ROS accumulation and cell death in rice. *Plant J.* **2020**, *105*, 942–956. [CrossRef] [PubMed]
4. Hu, G.; Richter, T.E.; Hulbert, S.H.; Pryor, T. Disease Lesion Mimicry Caused by Mutations in the Rust Resistance Gene rp1. *Plant Cell* **1996**, *8*, 1367–1376. [CrossRef]
5. Wu, C.; Bordeos, A.; Madamba, M.R.S.; Baraoidan, M.; Ramos, M.; Wang, G.-L.; Leach, J.E.; Leung, H. Rice lesion mimic mutants with enhanced resistance to diseases. *Mol. Genet. Genom.* **2008**, *279*, 605–619. [CrossRef] [PubMed]
6. Cai, L.; Yan, M.; Yun, H.; Tan, J.; Du, D.; Sun, H.; Guo, Y.; Sang, X.; Zhang, C. Identification and fine mapping of lesion mimic mutant *spl36* in rice (*Oryza sativa* L.). *Breed. Sci.* **2021**, *71*, 510–519. [CrossRef]
7. Kelly, D.; Vatsa, A.; Mayham, W.; Kazic, T. Extracting complex lesion phenotypes in *Zea mays*. *Mach. Vis. Appl.* **2015**, *27*, 145–156. [CrossRef]
8. Shirsekar, G.S.; Vega-Sanchez, M.E.; Bordeos, A.; Baraoidan, M.; Swisshelm, A.; Fan, J.; Park, C.H.; Leung, H.; Wang, G.-L. Identification and characterization of suppressor mutants of *spl11*-mediated cell death in rice. *Mol. Plant-Microbe Interact.* **2014**, *27*, 528–536. [CrossRef]
9. Hoisington, D.; Neuffer, M.; Walbot, V. Disease lesion mimics in maize: I. Effect of genetic background, temperature, developmental age, and wounding on necrotic spot formation with *Les1*. *Dev. Biol.* **1982**, *93*, 381–388. [CrossRef]
10. Wolter, M.; Hollricher, K.; Salamini, F.; Schulze-Lefert, P. The mlo resistance alleles to powdery mildew infection in barley trigger a developmentally controlled defence mimic phenotype. *Mol. Genet. Genom.* **1993**, *239*, 122–128. [CrossRef]
11. Yao, Q.; Zhou, R.; Fu, T.; Wu, W.; Zhu, Z.; Li, A.; Jia, J. Characterization and mapping of complementary lesion-mimic genes *lm1* and *lm2* in common wheat. *Theor. Appl. Genet.* **2009**, *119*, 1005–1012. [CrossRef] [PubMed]
12. Spassieva, S.; Hille, J. A lesion mimic phenotype in tomato obtained by isolating and silencing an *Lls1* homologue. *Plant Sci.* **2002**, *162*, 543–549. [CrossRef]

13. Wang, S.-H.; Lim, J.-H.; Kim, S.-S.; Cho, S.-H.; Yoo, S.-C.; Koh, H.-J.; Sakuraba, Y.; Paek, N.-C. Mutation of *SPOTTED LEAF3* (*SPL3*) impairs abscisic acid-responsive signalling and delays leaf senescence in rice. *J. Exp. Bot.* **2015**, *66*, 7045–7059. [CrossRef] [PubMed]
14. Tsuda, K.; Katagiri, F. Comparing signaling mechanisms engaged in pattern-triggered and effector-triggered immunity. *Curr. Opin. Plant Biol.* **2010**, *13*, 459–465. [CrossRef]
15. Nurnberger, T.; Brunner, F.; Kemmerling, B.; Piater, L. Innate immunity in plants and animals: Striking similarities and obvious differences. *Immunol. Rev.* **2004**, *198*, 249–266. [CrossRef]
16. Yuchun, R.A.O.; Ran, J.I.A.O.; Sheng, W.A.N.G.; Xianmei, W.U.; Hanfei, Y.E.; Chenyang, P.A.N.; Sanfeng, L.I.; Dedong, X.; Weiyong, Z.H.O.U.; Gaoxing, D.A.I.; et al. *SPL36* Encodes a Receptor-like Protein Kinase that Regulates Programmed Cell Death and Defense Responses in Rice. *Rice* **2021**, *14*, 34. [CrossRef]
17. Sun, H.; Mao, J.; Lan, B.; Zhang, C.; Zhao, C.; Pan, G.; Pan, X. Characterization and mapping of a spotted-leaf genotype, spl (*Y181*) that confers blast susceptibility in rice. *Eur. J. Plant Pathol.* **2014**, *140*, 407–417. [CrossRef]
18. Yin, Z.; Chen, J.; Zeng, L.; Goh, M.; Leung, H.; Khush, G.S.; Wang, G.-L. Characterizing rice lesion mimic mutants and identifying a mutant with broad-spectrum resistance to rice blast and bacterial blight. *Mol. Plant-Microbe Interact.* **2000**, *13*, 869–876. [CrossRef]
19. Shang, H.; Li, P.; Zhang, X.; Xu, X.; Gong, J.; Yang, S.; He, Y.; Wu, J.-L. The Gain-of-Function Mutation, *OsSpl26*, Positively Regulates Plant Immunity in Rice. *Int. J. Mol. Sci.* **2022**, *23*, 14168. [CrossRef]
20. Wang, L.; Han, S.; Zhong, S.; Wei, H.; Zhang, Y.; Zhao, Y.; Liu, B. Characterization and fine mapping of a necrotic leaf mutant in maize (*Zea mays* L.). *J. Genet. Genom.* **2013**, *40*, 307–314. [CrossRef]
21. Wang, S.; Wu, K.; Yuan, Q.; Liu, X.; Liu, Z.; Lin, X.; Zeng, R.; Zhu, H.; Dong, G.; Qian, Q.; et al. Control of grain size, shape and quality by *OsSPL16* in rice. *Nat. Genet.* **2012**, *44*, 950–954. [CrossRef] [PubMed]
22. Mori, M.; Tomita, C.; Sugimoto, K.; Hasegawa, M.; Hayashi, N.; Dubouzet, J.G.; Ochiai, H.; Sekimoto, H.; Hirochika, H.; Kikuchi, S. Isolation and molecular characterization of a Spotted leaf 18 mutant by modified activation-tagging in rice. *Plant Mol. Biol.* **2007**, *63*, 847–860. [CrossRef] [PubMed]
23. Zhou, Q.; Zhang, Z.; Liu, T.; Gao, B.; Xiong, X. Identification and Map-Based Cloning of the Light-Induced Lesion Mimic Mutant 1 (*LIL1*) Gene in Rice. *Front. Plant Sci.* **2017**, *8*, 2122. [CrossRef] [PubMed]
24. Kojo, K.; Yaeno, T.; Kusumi, K.; Matsumura, H.; Fujisawa, S.; Terauchi, R.; Iba, K. Regulatory mechanisms of ROI generation are affected by rice spl mutations. *Plant Cell Physiol.* **2006**, *47*, 1035–1044. [CrossRef] [PubMed]
25. Wang, Q.-L.; Sun, A.-Z.; Chen, S.-T.; Chen, L.-S.; Guo, F.-Q. *SPL6* represses signalling outputs of ER stress in control of panicle cell death in rice. *Nat. Plants* **2018**, *4*, 280–288. [CrossRef]
26. Huang, S.; Van Aken, O.; Schwarzländer, M.; Belt, K.; Millar, A.H. The Roles of Mitochondrial Reactive Oxygen Species in Cellular Signaling and Stress Response in Plants. *Plant Physiol.* **2016**, *171*, 1551–1559. [CrossRef]
27. Dickman, M.B.; Fluhr, R. Centrality of host cell death in plant-microbe interactions. *Annu. Rev. Phytopathol.* **2013**, *51*, 543–570. [CrossRef]
28. Wang, L.; Pei, Z.; Tian, Y.; He, C. *OsLSD1*, a rice zinc finger protein, regulates programmed cell death and callus differentiation. *Mol. Plant-Microbe Interact.* **2005**, *18*, 375–384. [CrossRef]
29. Zeng, L.-R.; Qu, S.; Bordeos, A.; Yang, C.; Baraoidan, M.; Yan, H.; Xie, Q.; Nahm, B.H.; Leung, H.; Wang, G.-L. *Spotted leaf11*, a negative regulator of plant cell death and defense, encodes a U-box/armadillo repeat protein endowed with E3 ubiquitin ligase activity. *Plant Cell* **2004**, *16*, 2795–2808. [CrossRef]
30. Hu, P.; Tan, Y.; Wen, Y.; Fang, Y.; Wang, Y.; Wu, H.; Wang, J.; Wu, K.; Chai, B.; Zhu, L.; et al. LMPA Regulates Lesion Mimic Leaf and Panicle Development Through ROS-Induced PCD in Rice. *Front. Plant Sci.* **2022**, *13*, 875038. [CrossRef]
31. Pei, Z.-M.; Murata, Y.; Benning, G.; Thomine, S.; Klüsener, B.; Allen, G.J.; Grill, E.; Schroeder, J.I. Calcium channels activated by hydrogen peroxide mediate abscisic acid signalling in guard cells. *Nature* **2000**, *406*, 731–734. [CrossRef] [PubMed]
32. Girotti, A.W. Photosensitized oxidation of membrane lipids: Reaction pathways, cytotoxic effects, and cytoprotective mechanisms. *J. Photochem. Photobiol. B Biol.* **2001**, *63*, 103–113. [CrossRef] [PubMed]
33. Rebeiz, C.A.; Montazer-Zouhoor, A.; Mayasich, J.M.; Tripathy, B.C.; Wu, S.; Rebeiz, C.C.; Friedmann, H.C. Photodynamic herbicides. Recent developments and molecular basis of selectivity. *Crit. Rev. Plant Sci.* **1988**, *6*, 385–436. [CrossRef]
34. Apel, K.; Hirt, H. Reactive oxygen species: Metabolism, oxidative stress, and signal transduction. *Annu. Rev. Plant Biol.* **2004**, *55*, 373–399. [CrossRef] [PubMed]
35. Hu, S.; Yu, Y.; Chen, Q.; Mu, G.; Shen, Z.; Zheng, L. *OsMYB45* plays an important role in rice resistance to cadmium stress. *Plant Sci.* **2017**, *264*, 1–8. [CrossRef]
36. Foyer, C.H.; Noctor, G. Redox homeostasis and antioxidant signaling: A metabolic interface between stress perception and physiological responses. *Plant Cell* **2005**, *17*, 1866–1875. [CrossRef]
37. Chai, T.; Zhou, J.; Liu, J.; Xing, D. *LSD1* and *HY5* antagonistically regulate red light induced-programmed cell death in Arabidopsis. *Front. Plant Sci.* **2015**, *6*, 292. [CrossRef]
38. Abou-Attia, M.A.; Wang, X.; Al-Attala, M.N.; Xu, Q.; Zhan, G.; Kang, Z. *TaMDAR6* acts as a negative regulator of plant cell death and participates indirectly in stomatal regulation during the wheat stripe rust-fungus interaction. *Physiol. Plant.* **2015**, *156*, 262–277. [CrossRef]

39. Xiao, G.; Zhou, J.; Lu, X.; Huang, R.; Zhang, H. Excessive UDPG resulting from the mutation of *UAP1* causes programmed cell death by triggering reactive oxygen species accumulation and caspase-like activity in rice. *New Phytol.* **2017**, *217*, 332–343. [CrossRef]
40. Yang, C.; Li, W.; Cao, J.; Meng, F.; Yu, Y.; Huang, J.; Jiang, L.; Liu, M.; Zhang, Z.; Chen, X.; et al. Activation of ethylene signaling pathways enhances disease resistance by regulating ROS and phytoalexin production in rice. *Plant J.* **2017**, *89*, 338–353. [CrossRef]
41. Wang, S.; Lei, C.; Wang, J.; Ma, J.; Tang, S.; Wang, C.; Zhao, K.; Tian, P.; Zhang, H.; Qi, C.; et al. *SPL33*, encoding an eEF1A-like protein, negatively regulates cell death and defense responses in rice. *J. Exp. Bot.* **2017**, *68*, 899–913. [CrossRef] [PubMed]
42. Tsukagoshi, H.; Busch, W.; Benfey, P.N. Transcriptional regulation of ROS controls transition from proliferation to differentiation in the root. *Cell* **2010**, *143*, 606–616. [CrossRef]
43. Silva-Navas, J.; Moreno-Risueno, M.A.; Manzano, C.; Téllez-Robledo, B.; Navarro-Neila, S.; Carrasco, V.; Pollmann, S.; Gallego, F.J.; del Pozo, J.C. Flavonols Mediate Root Phototropism and Growth through Regulation of Proliferation-to-Differentiation Transition. *Plant Cell* **2016**, *28*, 1372–1387. [CrossRef] [PubMed]
44. Manzano, C.; Pallero-Baena, M.; Casimiro, I.; De Rybel, B.; Orman-Ligeza, B.; Van Isterdael, G.; Beeckman, T.; Draye, X.; Casero, P.; del Pozo, J.C. The Emerging Role of Reactive Oxygen Species Signaling during Lateral Root Development. *Plant Physiol.* **2014**, *165*, 1105–1119. [CrossRef] [PubMed]
45. Clore, A.M.; Doore, S.M.; Tinnirello, S.M.N. Increased levels of reactive oxygen species and expression of a cytoplasmic aconitase/iron regulatory protein 1 homolog during the early response of maize pulvini to gravistimulation. *Plant Cell Environ.* **2007**, *31*, 144–158. [CrossRef] [PubMed]
46. Joo, J.H.; Bae, Y.S.; Lee, J.S. Role of auxin-induced reactive oxygen species in root gravitropism. *Plant Physiol.* **2001**, *126*, 1055–1060. [CrossRef] [PubMed]
47. Chen, X.; Hao, L.; Pan, J.; Zheng, X.; Jiang, G.; Jin, Y.; Gu, Z.; Qian, Q.; Zhai, W.; Ma, B. *SPL5*, a cell death and defense-related gene, encodes a putative splicing factor 3b subunit 3 (SF3b3) in rice. *Mol. Breed.* **2011**, *30*, 939–949. [CrossRef]
48. Wellburn, A.R. The Spectral Determination of Chlorophylls a and b, as well as Total Carotenoids, Using Various Solvents with Spectrophotometers of Different Resolution. *J. Plant Physiol.* **1994**, *144*, 307–313. [CrossRef]
49. Han, S.-H.; Sakuraba, Y.; Koh, H.-J.; Paek, N.-C. Leaf variegation in the rice *zebra2* mutant is caused by photoperiodic accumulation of tetra-Cis-lycopene and singlet oxygen. *Mol. Cells* **2011**, *33*, 87–97. [CrossRef]
50. Leshem, Y.; Melamed-Book, N.; Cagnac, O.; Ronen, G.; Nishri, Y.; Solomon, M.; Cohen, G.; Levine, A. Suppression of *Arabidopsis* vesicle-SNARE expression inhibited fusion of H_2O_2-containing vesicles with tonoplast and increased salt tolerance. *Proc. Natl. Acad. Sci. USA* **2006**, *103*, 18008–18013. [CrossRef]
51. Li, Z.; Zhang, Y.; Liu, L.; Liu, Q.; Bi, Z.; Yu, N.; Cheng, S.; Cao, L. Fine mapping of the lesion mimic and early senescence 1 *(lmes1)* in rice (*Oryza sativa*). *Plant Physiol. Biochem.* **2014**, *80*, 300–307. [CrossRef] [PubMed]
52. Hess, W.R.; Börner, T. Organellar RNA polymerases of higher plants. *Int. Rev. Cytol.* **1999**, *190*, 1–59. [CrossRef] [PubMed]
53. Shiina, T.; Tsunoyama, Y.; Nakahira, Y.; Khan, M.S. Plastid RNA polymerases, promoters, and transcription regulators in higher plants. *Int. Rev. Cytol.* **2005**, *244*, 1–68. [CrossRef] [PubMed]
54. He, L.; Zhang, S.; Qiu, Z.; Zhao, J.; Nie, W.; Lin, H.; Zhu, Z.; Zeng, D.; Qian, Q.; Zhu, L. FRUCTOKINASE-LIKE PROTEIN 1 interacts with TRXz to regulate chloroplast development in rice. *J. Integr. Plant Biol.* **2018**, *60*, 94–111. [CrossRef]
55. Takeuchi, R.; Kimura, S.; Saotome, A.; Sakaguchi, K. Biochemical properties of a plastidial DNA polymerase of rice. *Plant Mol. Biol.* **2007**, *64*, 601–611. [CrossRef]
56. Qiao, Y.; Jiang, W.; Lee, J.; Park, B.; Choi, M.; Piao, R.; Woo, M.; Roh, J.; Han, L.; Paek, N.; et al. *SPL28* encodes a clathrin-associated adaptor protein complex 1, medium subunit µ1 (AP1M1) and is responsible for spotted leaf and early senescence in rice (*Oryza sativa*). *New Phytol.* **2009**, *185*, 258–274. [CrossRef]
57. Zhao, M.; Guo, Y.; Sun, H.; Dai, J.; Peng, X.; Wu, X.; Yun, H.; Zhang, L.; Qian, Y.; Li, X.; et al. Lesion mimic mutant 8 balances disease resistance and growth in rice. *Front. Plant Sci.* **2023**, *14*, 1189926. [CrossRef]
58. Ma, J.; Wang, Y.; Ma, X.; Meng, L.; Jing, R.; Wang, F.; Wang, S.; Cheng, Z.; Zhang, X.; Jiang, L.; et al. Disruption of gene *SPL35*, encoding a novel CUE domain-containing protein, leads to cell death and enhanced disease response in rice. *Plant Biotechnol. J.* **2019**, *17*, 1679–1693. [CrossRef]
59. Yang, Y.; Qi, M.; Mei, C. Endogenous salicylic acid protects rice plants from oxidative damage caused by aging as well as biotic and abiotic stress. *Plant J.* **2004**, *40*, 909–919. [CrossRef]
60. Kang, S.G.; Lee, K.E.; Singh, M.; Kumar, P.; Matin, M.N. Rice Lesion Mimic Mutants (LMM): The Current Understanding of Genetic Mutations in the Failure of ROS Scavenging during Lesion Formation. *Plants* **2021**, *10*, 1598. [CrossRef]
61. Yamada, M.; Han, X.; Benfey, P.N. *RGF1* controls root meristem size through ROS signalling. *Nature* **2020**, *577*, 85–88. [CrossRef] [PubMed]
62. Dunand, C.; Crèvecoeur, M.; Penel, C. Distribution of superoxide and hydrogen peroxide in *Arabidopsis* root and their influence on root development: Possible interaction with peroxidases. *New Phytol.* **2007**, *174*, 332–341. [CrossRef] [PubMed]
63. Berthold, D.A.; Voevodskaya, N.; Stenmark, P.; Gräslund, A.; Nordlund, P. EPR studies of the mitochondrial alternative oxidase: Evidence for a diiron carboxylate center. *Perspect. Surg.* **2002**, *277*, 43608–43614. [CrossRef]
64. Affourtit, C.; Albury, M.S.; Crichton, P.G.; Moore, A.L. Exploring the molecular nature of alternative oxidase regulation and catalysis. *FEBS Lett.* **2001**, *510*, 121–126. [CrossRef]

65. Li, H.; Zhang, H.; Yang, Y.; Fu, G.; Tao, L.; Xiong, J. Effects and oxygen-regulated mechanisms of water management on cadmium (Cd) accumulation in rice (*Oryza sativa*). *Sci. Total Environ.* **2022**, *846*, 157484. [CrossRef]
66. Murakami, Y.; Toriyama, K. Enhanced high temperature tolerance in transgenic rice seedlings with elevated levels of alternative oxidase, *OsAOX1a*. *Plant Biotechnol.* **2008**, *25*, 361–364. [CrossRef]
67. Vanlerberghe, G.C.; Cvetkovska, M.; Wang, J. Is the maintenance of homeostatic mitochondrial signaling during stress a physiological role for alternative oxidase? *Physiol. Plant.* **2009**, *137*, 392–406. [CrossRef]
68. Saika, H.; Ohtsu, K.; Hamanaka, S.; Nakazono, M.; Tsutsumi, N.; Hirai, A. *AOX1c*, a novel rice gene for alternative oxidase; Comparison with rice AOX1a and AOX1b. *Genes Genet. Syst.* **2002**, *77*, 31–38. [CrossRef]
69. Guan, Q.; Takano, T.; Liu, S. Genetic transformation and analysis of rice *OsAPx2* gene in *Medicago sativa*. *PLoS ONE* **2012**, *7*, e41233. [CrossRef]
70. Lin, A.; Wang, Y.; Tang, J.; Xue, P.; Li, C.; Liu, L.; Hu, B.; Yang, F.; Loake, G.J.; Chu, C. Nitric oxide and protein *S*-nitrosylation are integral to hydrogen peroxide-induced leaf cell death in rice. *Plant Physiol.* **2011**, *158*, 451–464. [CrossRef]
71. Zheng, Y.; Xu, J.; Wang, F.; Tang, Y.; Wei, Z.; Ji, Z.; Wang, C.; Zhao, K. Mutation Types of *CYP71P1* Cause Different Phenotypes of Mosaic Spot Lesion and Premature Leaf Senescence in Rice. *Front. Plant Sci.* **2021**, *12*, 641300. [CrossRef] [PubMed]
72. Das, B.K.; Xia, L.; Palandjian, L.; Gozani, O.; Chyung, Y.; Reed, R. Characterization of a protein complex containing spliceosomal proteins SAPs 49, 130, 145, and 155. *Mol. Cell. Biol.* **1999**, *19*, 6796–6802. [CrossRef] [PubMed]
73. Golas, M.M.; Sander, B.; Will, C.L.; Lührmann, R.; Stark, H. Molecular architecture of the multiprotein splicing factor SF3b. *Science* **2003**, *300*, 980–984. [CrossRef] [PubMed]
74. Menon, S.; Tsuge, T.; Dohmae, N.; Takio, K.; Wei, N. Association of SAP130/SF3b-3 with Cullin-RING ubiquitin ligase complexes and its regulation by the COP9 signalosome. *BMC Biochem.* **2008**, *9*, 1. [CrossRef]
75. Yamasaki, S.; Ishikawa, E.; Sakuma, M.; Hara, H.; Ogata, K.; Saito, T. Mincle is an ITAM-coupled activating receptor that senses damaged cells. *Nat. Immunol.* **2008**, *9*, 1179–1188. [CrossRef]
76. Jincho, Y.; Sotomaru, Y.; Kawahara, M.; Ono, Y.; Ogawa, H.; Obata, Y.; Kono, T. Identification of genes aberrantly expressed in mouse embryonic stem cell-cloned blastocysts. *Biol. Reprod.* **2008**, *78*, 568–576. [CrossRef]
77. Ge, C.-W.; E, Z.-G.; Pan, J.-J.; Jiang, H.; Zhang, X.-Q.; Zeng, D.-L.; Dong, G.-J.; Hu, J.; Xue, D.-W. Map-based cloning of a spotted-leaf mutant gene *OsSL5* in Japonica rice. *Plant Growth Regul.* **2014**, *75*, 595–603. [CrossRef]